RESEARCH ARTICLE

Design and Development of Nanoparticulate Dosage Form of Ivacaftor for Treatment of Cystic Fibrosis

Bhavesh Mali[1], Kandukuri Sushma[1*], Himanshu Patel[1], Nidhi Raichura[2]

[1]*Department of Pharmaceutics, Parul University, Vadodara, Gujarat-391760, India*
[2]*Department of Pharmaceutical Chemistry, Parul University, Vadodara, Gujarat-391760, India*

Received: 21st Jun, 2025; Revised: 1st Aug, 2025; Accepted: 14th Aug, 2025; Available Online: 25th Sep, 2025

ABSTRACT

Objective: This study aimed to develop Ivacaftor-loaded Poly(lactic-co-glycolic acid) (PLGA) nanoparticles to enhance drug solubility, pulmonary delivery, and therapeutic efficacy in CF patients.

Methods: PLGA was used to prepare Ivacaftor nanoparticles by the single-emulsion solvent evaporation method, using polyvinyl alcohol (PVA) as a stabilizer and a solvent system of ethanol and dichloromethane. Optimization of the formulation was carried out by changing the polymer-to-drug ratios, surfactant concentration, homogenization speed and time of sonication. The characterization of the produced nanoparticles, including particle size, polydispersity index, encapsulation efficiency, kinetics of drug release, and stability, was assessed.

Results: The optimized formulation achieved high encapsulation efficiency alongside a narrow size distribution and mean particle size that was tailored for pulmonary administration. *In vitro* drug release studies showed sustained release of the drug, exhibiting zero-order kinetics. Stability studies confirmed the physical and chemical stability of the nanoparticles over the duration of the storage period.

Conclusion: The PLGA nanoparticulate system containing Ivacaftor, developed in this study, holds potential for targeted pulmonary delivery in cystic fibrosis therapies. The system is designed to improve solubility and enable controlled drug release, thereby increasing bioavailability, reducing systemic exposure, and improving patient adherence through less frequent dosing. Further investigations, both *in vivo* and clinical, are needed to establish its therapeutic promise.

Keywords: nanoparticulate system, Ivacaftor, Cystic Fibrosis, PLGA

How to cite this article: Bhavesh Mali, Kandukuri Sushma, Himanshu Patel, Nidhi Raichura. Design and Development of Nanoparticulate Dosage Form of Ivacaftor for Treatment of Cystic Fibrosis. International Journal of Drug Delivery Technology. 2025;15(3):1119-29. doi: 10.25258/ijddt.15.3.30

Source of support: RDC Cell, Parul University.

Conflict of interest: None

INTRODUCTION

Ivacaftor is a CFTR (cystic fibrosis transmembrane conductance regulator) potentiator prescribed for patients with specific gating mutations of cystic fibrosis (CF)[1,2]. With its clinical effectiveness, Ivacaftor is still challenged by poor aqueous solubility and low bioavailability, which require frequent dosing and consistent therapeutic outcomes[3,4]. A promising approach to overcome the solubility, dissolution rate, and absorption challenges of poorly water soluble drugs like Ivacaftor is nanotechnology applied to drug delivery systems[5]. Such systems improve drug stability and controlled release as well as provide targeted delivery, thereby increasing therapeutic efficacy and reducing systemic side effects[6]. This study seeks to design and develop a nanoparticulate dosage form of Ivacaftor in order to effectively treat cystic fibrosis bypassing its biopharmaceutical Limitations.

MATERIALS AND METHODS

Materials

Ivacaftor was obtained from Alembic Pharmaceuticals, and PLGA (50:50) from Nomisma Healthcare. PVA, DCM, and ethanol were sourced from SRL and Ureca Consumer Co-Op. Stores Ltd., respectively. All reagents used were of analytical grade unless specified.

Method of Preparation of Nanoparticle

Ivacaftor-loaded PLGA nanoparticles were prepared by dissolving the drug in ethanol and PLGA in dichloromethane to form an oil phase, which was emulsified into an aqueous phase under high-speed homogenization. The resulting emulsion was probe-sonicated (45% amplitude, 2-sec pulses) for nanoscale size reduction, followed by centrifugation at 15,000 rpm for 30 minutes. The nanoparticles were washed twice with distilled water and freeze-dried to yield a stable powder, ensuring efficient drug encapsulation and improved bioavailability[7-10].

Preparation of Stock Solution

The drug was prepared in the form of a stock solution by dissolving 10 mg in 10 mL of ethanol, which resulted in a concentration of 1000 µg/mL. This stock solution was further diluted to achieve a working concentration of 10 µg/mL. The concentration of the 10 µg/mL solution was further analyzed through UV spectrophotometry in the wavelength range of 200-400 nm.

Preparation of Calibration Curve of Ivacaftor in Ethanol

**Author for Correspondence: Sushma.kandukuri121132@paruluniveristy.ac.in*

Table 1: Levels of Independent Factors in 3-Level 2-Factor

Level	Variable	
	X1 = Drug-Polymer Ratio	X2 = Sonication Time
-1	1:3	15
0	1:5	20
+1	1:7	25

Table 2: Insignia of Independent and Dependent Variable

Independent Variable Codes	Factor Selected
X_1	Drug: Polymer
X_2	Sonication Time
Dependent Variable Codes	Dependent variables selected for optimization
Y_1	Particle Size (nm)
Y_2	% Entrapment Efficiency
Y_3	% CDR (24hrs)

Aliquots from the stock solution are transferred into separate volumetric flasks and diluted with ethanol to a final volume of 10 mL, resulting in concentrations of 1, 2,3, 4, 5, 6, and 7 µg/mL. The absorbance of these solutions is measured at 247 nm using a UV spectrophotometer. A calibration curve is then constructed by plotting the concentrations on the X-axis against the corresponding absorbance values on the Y-axis to generate the standard curve**.**

Preparation of Calibration Curve of Ivacaftor in Saline Phosphate Buffer (7.4 pH)

Aliquots from the stock solution are transferred into separate volumetric flasks and diluted with ethanol to a final volume of 10 mL, resulting in concentrations of 2, 4, 6, 8, 10, 12, and 14 µg/mL. The absorbance of these solutions is measured at 247 nm using a UV spectrophotometer. A calibration curve is then constructed by plotting the concentrations on the X-axis against the corresponding absorbance values on the Y-axis to generate the standard curve.

Experimental Design

A two-factor, three-level experimental design enables the systematic evaluation of two independent variables, each at three levels, to assess their individual and interactive effects on dependent responses. This design, generating nine experimental runs, captures non-linear relationships and supports response surface modeling. In this study, it was applied to optimize Ivacaftor-loaded polymeric nanoparticles, using sonication time and drug-polymer concentration as independent variables, and % entrapment efficiency, particle size, and % cumulative drug release (CDR) as responses (Tables 2 and 3)[11].

Table 3: 3-Level 2-Factor Experimental Design

Std	Run	Factor 1 (X1)		Factor 2 (X2)	
1	9	-1	1:3	-1	15
2	3	0	1:5	-1	15
3	6	+1	1:7	-1	15
4	1	-1	1:3	0	20
5	8	0	1:5	0	20
6	5	+1	1:7	0	20
7	7	-1	1:3	+1	25
8	2	0	1:5	+1	25
9	4	+1	1:7	+1	25

Table 4: Solubility of Ivacaftor was evaluated in various solvents

S. No.	Solvents	Solubility	Interpretation
1	Water	0.005 ± 0.34	Insoluble
2	Ethanol	21.96 ± 0.21	Freely Soluble
3	Methanol	12.16 ± 0.21	Soluble
4	Dichloromethane	8.09 ± 0.48	Soluble
5	7.4 pH SPB	9.51 ± 0.52	Soluble

Table 5: Analysis Result of FT-IR Spectrum

S. No.	Observed peck (cm^{-1})		Reference Range (cm^{-1})	Functional Group
	Drug	Drug: Polymer		
1	3284.64	3284.05	3250-3500	N-H
2	3110.24	3087.60	2700-3200	O-H
3	2958.64	2954.52	2850-3000	C-H
4	1521.47	1524.99	1500-1600	C=C
5	1639.40	1646.21	1590-1650	C=O

Characterisation

Pre-formulation Studies

Identification of the Drug

The Physical Appearance, Nature, Odour, and Color of the drug were characterized by using descriptive technology.

Melting Point

The melting point refers to the temperature range at which a solid transition into a liquid state. The melting point of Ivacaftor was determined using a melting point apparatus. A small quantity of the drug was placed inside a capillary tube, which was then inserted into the apparatus. The temperature at which the drug began to melt was recorded using a thermometer[12].

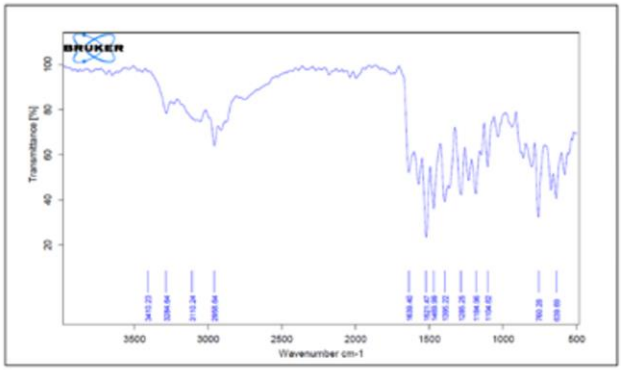

Figure 1: FT-IR of Ivacaftor

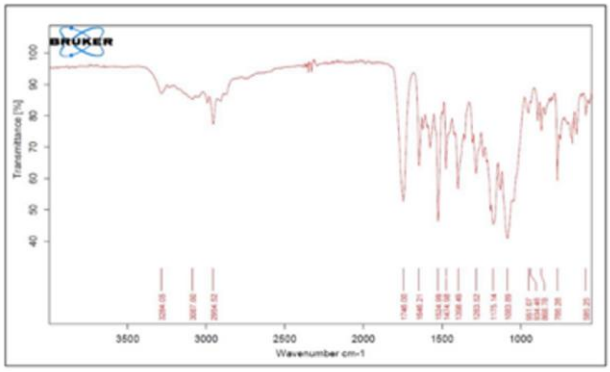

Figure 2: FT-IR of Ivacaftor-PLGA 50:50

Table 6: Absorbance of Ivacaftor in Ethanol and 7.4pH Saline Phosphate Buffer

Ethanol		7.4 pH Saline Phosphate Buffer	
Concentration (µg/mL)	Average Absorbance at 247 nm	Concentration (µg/mL)	Average Absorbance at 247 nm
1	0.152 ± 0.0032	2	0.138 ± 0.0056
2	0.301 ± 0.0036	4	0.244 ± 0.0044
3	0.443 ± 0.0026	6	0.396 ± 0.0031
4	0.511 ± 0.0047	8	0.507 ± 0.0026
5	0.673 ± 0.0015	10	0.641 ± 0.0017
6	0.804 ± 0.0028	12	0.783 ± 0.0055
7	0.914 ± 0.0045	14	0.899 ± 0.0048

Solubility Study

The Pre-formulation solubility analysis was performed by oversaturating the drug in glass vials containing 2 mL of Water, Methanol, Dichloromethane, Ethanol, and 7.4 pH Saline Phosphate Buffer. The supernatant solution was separated by cold centrifugation after 24 hours. Further adjustments in concentration were made through appropriate dilutions[13].

Drug Polymer Interaction

An FTIR spectrophotometer was used to analyze the characteristic peaks in the IR spectra of Ivacaftor and the polymer. The samples were stored for two weeks, after which their FTIR spectra were recorded to assess any potential interactions or changes in functional groups over time[14-18].

In-vitro Drug Release Study

The measurement will be conducted using a Franz diffusion cell. One compartment will contain Ivacaftor-loaded nanoparticles, while the other will hold a phosphate saline buffer with a pH of 7.4, as the drug has poor water solubility.

A dialysis membrane will be placed between the two compartments. The cells will be maintained at a constant temperature with continuous stirring. Over a 24-hour period, small samples of the solution will be collected at various intervals and replaced with fresh buffer to ensure consistent conditions. The collected samples will then be analyzed using UV spectroscopy at a wavelength of 247 nm[18-21].

Table 7: ANOVA for Quadratic Model

Run	Factor 1 (Drug: Polymer)	Factor 2 (Sonication Time)	Response 1 (%EE)	Response 2 (Particle Size)	Response 3 (%CDR)
1	1:3	15	61.6	356.5	80.7
2	1:5	15	74.75	362.9	83.7
3	1:7	15	73.4	417.5	93.3
4	1:3	20	66.6	310.6	87.7
5	1:5	20	78.05	330.9	89.3
6	1:7	20	79.05	331.2	85.5
7	1:3	25	69.6	244.1	79.9
8	1:5	25	83.3	282.8	89.8
9	1:7	25	86.4	312.8	86.4

Stability of Ivacaftor Loaded Nanoparticles

A stability study will be carried out following ICH guidelines. The stability of various formulations will be assessed after storing them at 25±2°C and 65%±5% relative humidity for one month. Samples will be collected after 30 days, and any variations in particle size and % CDR will be evaluated. The results will be presented as the mean ± standard deviation (S.D.) based on at least three measurements[22,23].

RESULTS

Organoleptic Evaluation

The organoleptic evaluation of the sample drug showed complete similarity with the reference standard. Both exhibited solid state, white to off-white color, odorless character, and crystalline nature. This confirms the physical consistency and identity of the sample.

Melting Point

The observed value obtained from the experimental determination of ivacaftor's melting point range is 291-295°C.

This observed range closely matches the theoretically reported value, with only a slight deviation of 1°C in the lower limit.

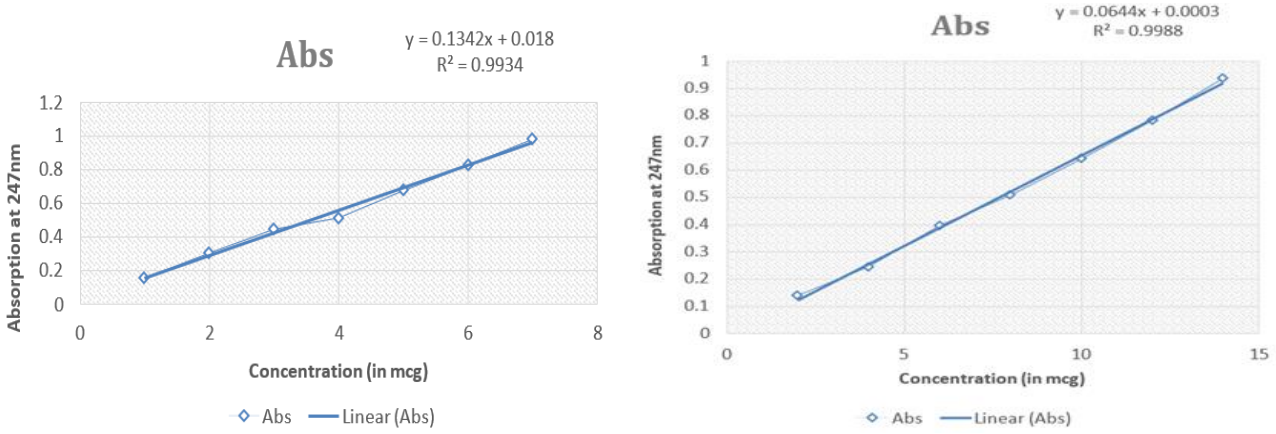

Figure 3: Calibration Curve of Ivacaftor in Ethanol and 7.4pH Saline Phosphate Buffer

Table 8: Summary of ANOVA table of % Entrapment Efficiency

Source	Sum of Squares	df	Mean Square	F Value	p-value (Prob > F)	Significance
Model	503.00	5	100.60	104.13	0.0015	Significant
A – PLGA	280.85	1	280.85	290.70	0.0004	
B – Sonication time	145.53	1	145.53	150.64	0.0012	
AB	6.25	1	6.25	6.47	0.0844	
A^2	70.21	1	70.21	72.67	0.0034	
B^2	0.15	1	0.15	0.16	0.7188	
Residual	2.90	3	0.97			
Cor Total	505.90	8				

Table 9: Summary of ANOVA table of % Particle Size

Source	Sum of Squares	df	Mean Square	F Value	p-value (Prob > F)	Significance
Model	18576.35	5	3715.27	10.15	0.0425	Significant
A - PLGA	3765.01	1	3765.01	10.29	0.0491	
B - Sonication time	14721.31	1	14721.31	40.22	0.0079	
AB	14.82	1	14.82	0.040	0.8534	
A^2	21.13	1	21.13	0.058	0.8256	
B^2	54.08	1	54.08	0.15	0.7263	
Residual	1098.05	3	366.02			
Cor Total	19674.40	8				

Table 10: Summary of ANOVA Table of % CDR

Source	Sum of Squares	df	Mean Square	F Value	p-value (Prob > F)	Significance
Model	492.43	5	98.49	20.80	0.0155	Significant
A – PLGA	285.66	1	285.66	60.32	0.0044	
B – Sonication time	41.61	1	41.61	8.79	0.0594	
AB	1.69	1	1.69	0.36	0.5923	
A^2	72.80	1	72.80	15.37	0.0295	
B^2	90.68	1	90.68	19.15	0.0221	
Residual	14.21	3	4.74			
Cor Total	506.64	8				

Solubility

Ivacaftor exhibited poor solubility in water, indicating its hydrophobic nature, while it was found to be freely soluble in ethanol and soluble in methanol, dichloromethane, and pH 7.4 phosphate buffer, as shown in Table 4. These findings support the need for a suitable delivery system to enhance its aqueous solubility and bioavailability.

FT-IR Spectroscopy

FT-IR analysis confirmed that the characteristic peaks of Ivacaftor—corresponding to N–H, O–H, C–H, C=C, and C=O stretching vibrations—were retained in the drug–polymer mixture, with all observed values falling within their respective reference ranges. No new peaks or shifts were observed, indicating the absence of significant chemical interactions and confirming drug–polymer compatibility (Table 5 and Figure 1,2).

UV Analytical Method

Preparation of Standard Calibration Curve in Ethanol and pH 7.4 Saline Phosphate Buffer

The standard calibration curve of Ivacaftor in ethanol was established over a concentration range of 1 to 7 µg/mL. The curve demonstrated linearity with a regression coefficient (R^2) close to 1 at 247 nm, indicating reliable absorbance-concentration correlation (Table 7 and Figure 3). Similarly, a calibration curve in pH 7.4 saline phosphate buffer was constructed for concentrations ranging from 2 to 14 µg/mL. This range also exhibited excellent linearity, with a regression coefficient near unity, confirming the suitability of the buffer system for quantitative analysis of Ivacaftor (Table 6 and Figure 3).

Table 11: Predicted value and observed value of %EE, Particle Size and %CDR

Batch	Parameters	Predicted Value	Experimental Value	% Relative Error
IN8	%EE	82.783	83.3	0.63
	Particle Size	290.545	282.8	2.67
	%CDR	85.6323	89.8	4.87

X-Ray Diffraction (XRD)

The study demonstrated that the crystallinity of Ivacaftor underwent a transformation into a partially amorphous state during the process of nanoparticle formulation. This structural alteration, as confirmed by X-ray diffraction (XRD) analysis, is believed to have significantly improved the drug's solubility and bioavailability. Consequently, this enhancement likely contributed to the increased therapeutic effectiveness of the Ivacaftor-loaded PLGA nanoparticles (Figure 4 and 5).

Screening of Parameters for Formulation

Preliminary studies were conducted to screen critical formulation parameters for the development of Ivacaftor-loaded polymeric nanoparticles. The effect of the drug-to-polymer ratio was evaluated across six ratios, with the 1:7 ratio showing optimal entrapment efficiency and a favorable polydispersity index (PDI), indicating efficient

drug loading and uniform particle distribution. The concentration of the surfactant (PVA) was optimized, and a concentration of 1% w/v was found to produce nanoparticles with the smallest and most desirable particle size, while higher concentrations led to increased size due to possible micelle formation. The RPM of the high-speed homogenizer was also assessed, where 900 RPM yielded the highest nanoparticle production efficiency. Finally, sonicator amplitude was varied, and 45% amplitude resulted in the lowest PDI with particle size below 500 nm, suggesting optimal energy input for nanoparticle formation. These findings provided a strong foundation for further optimization using a statistical experimental design.

Optimization of Formulation by 3^2 Full Factorial Design

Optimization of the nanoparticle formulation was carried out using a 3-level, 2-factor Full Factorial Design. This approach systematically examined the effects of the drug-to-polymer ratio and sonication time, selected as the independent variables, on critical formulation parameters such as particle size, entrapment efficiency, and cumulative drug release (%CDR). By exploring three levels of these factors, a robust dataset was generated, highlighting both individual and interaction effects (Table 8).

Table 12: % Yield, % DL and % EE of IN1 – IN

Batch	Nanoparticle Yield (%)	Drug Loading (%)	%EE
IN1	92.5	16.65	61.6
IN2	97.5	19.17	74.75
IN3	95	19.31	73.4
IN4	88.33	12.57	66.6
IN5	92.5	14.06	78.05
IN6	90.83	14.50	79
IN7	88.13	9.87	69.6
IN8	91.25	11.1	83.3
IN9	89.34	12.08	86.4

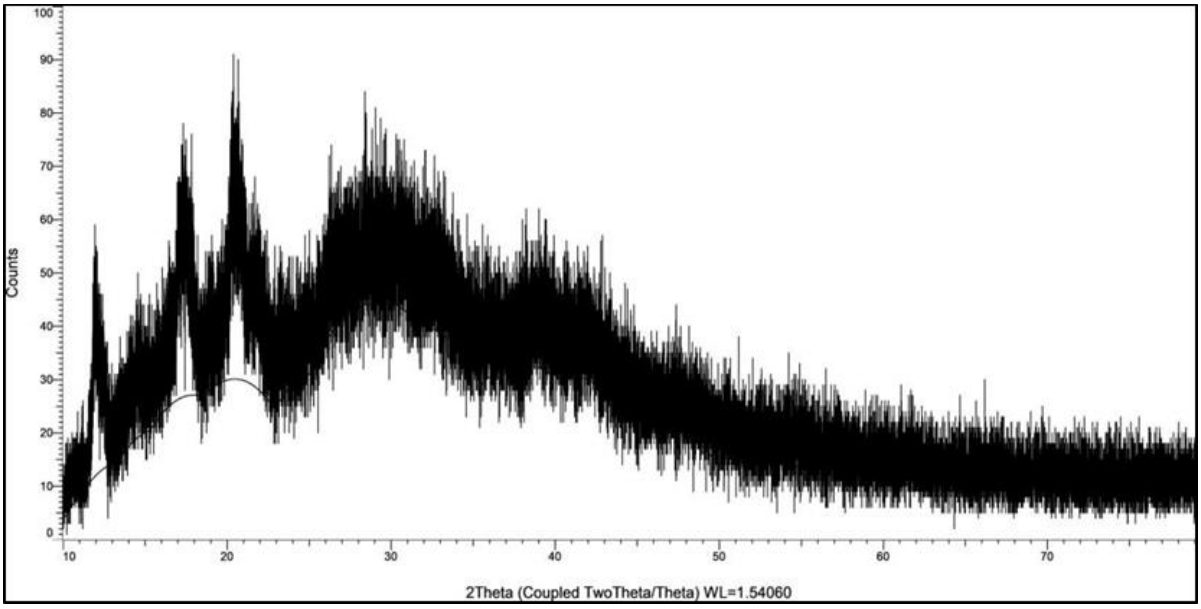

Figure 4: Crystallinity XRD graph of Drug with Polymer

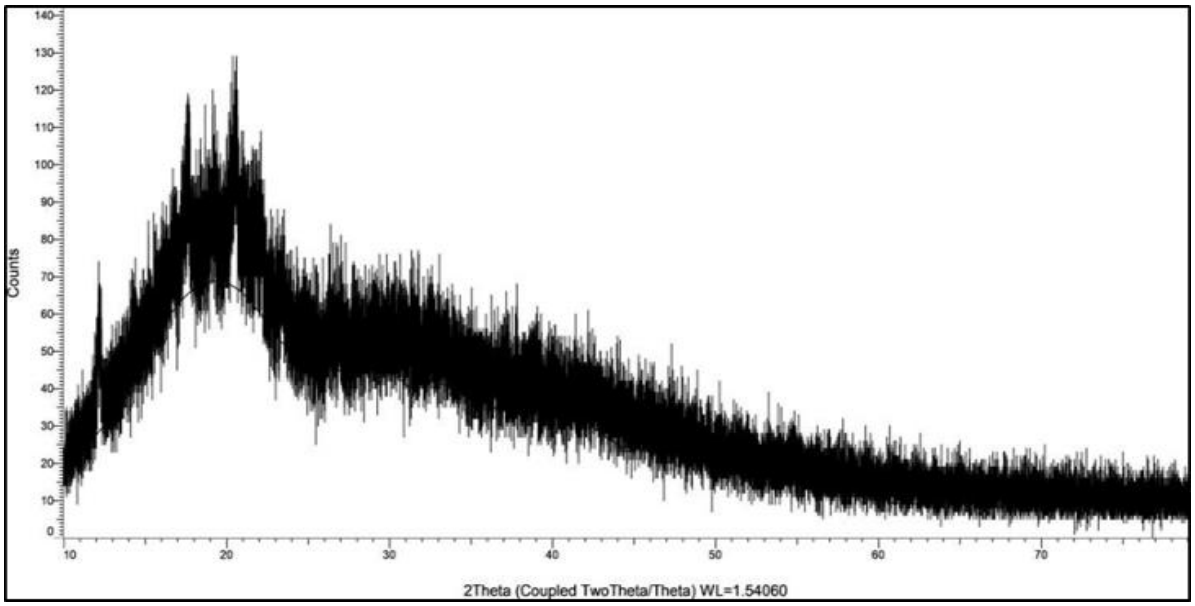

Figure 5: Partially Amorphous XRD graph of formulation

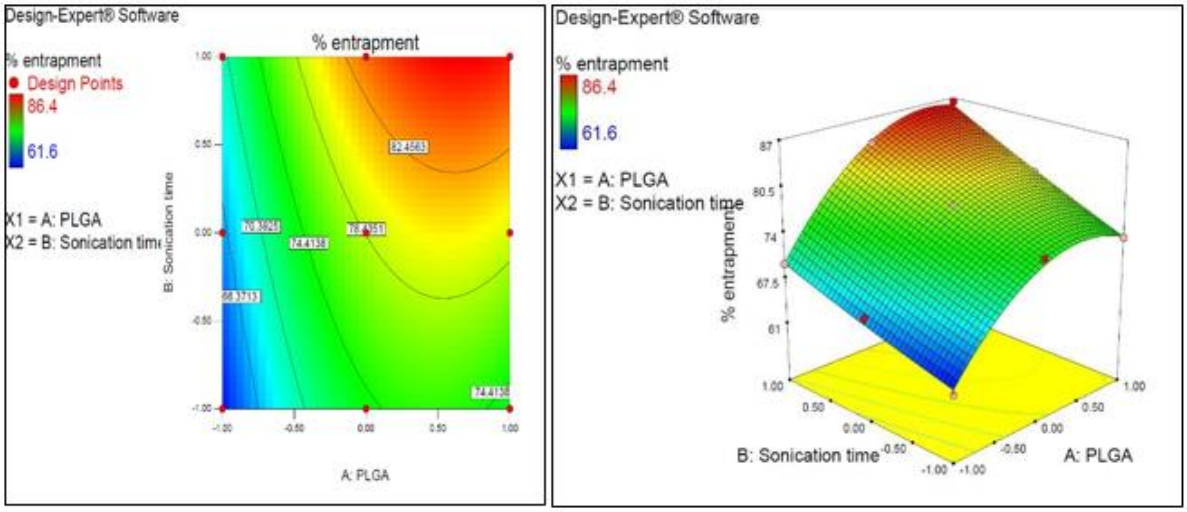

Figure 6: Counter and 3D Plot of %EE

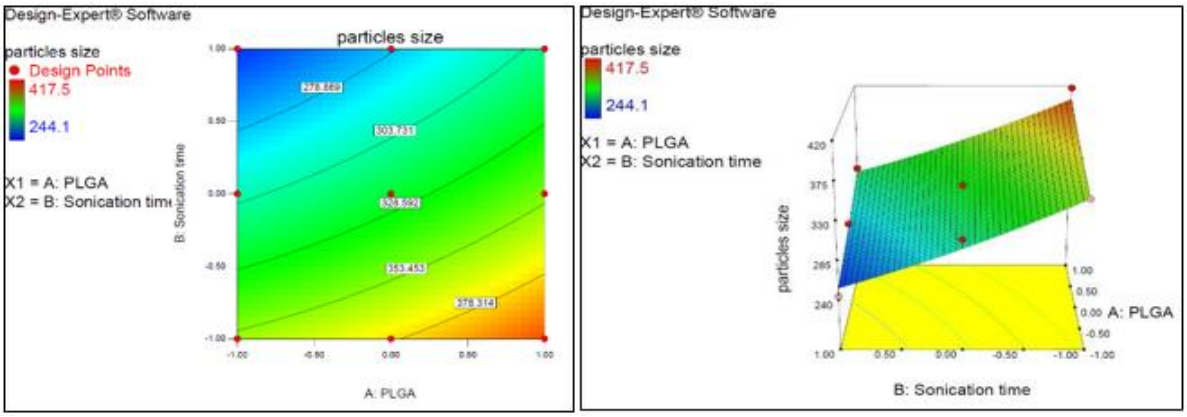

Figure 7: Counter and 3D Plot of % Particle Size

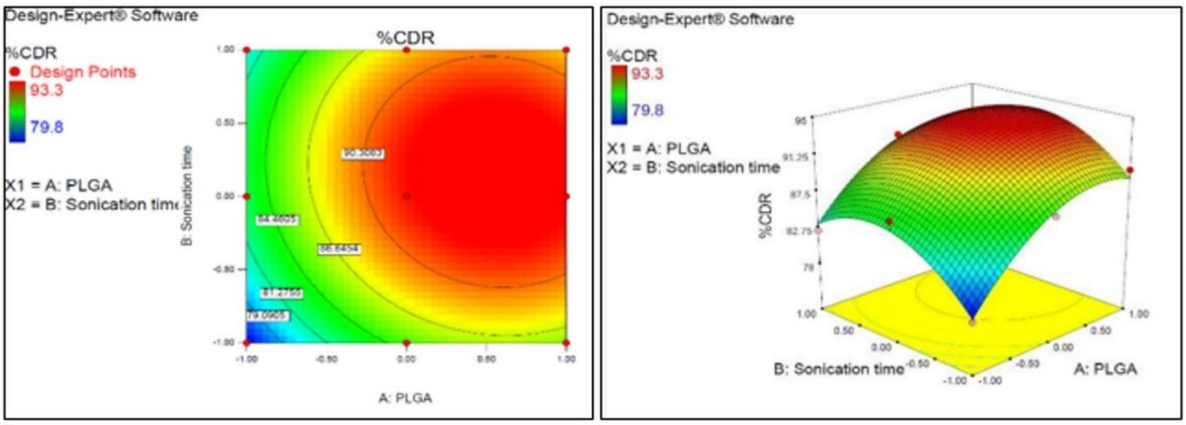

Figure 8: Counter and 3D Plot of % CDR

Response 1: % Entrapment Efficiency

The model was found to be statistically significant, indicating that the selected formulation factors had a meaningful impact on the response. PLGA concentration and sonication time were the major contributing variables. The quadratic effect of PLGA was also significant, while the interaction between variables showed no notable influence (Table 9 and Figures 6).

% Entrapment Efficiency = 78.52 + 6.84*A + 4.92*B + 1.25*A*B – 5.92*A2 + 0.28*B2

Response 2: Particle Size

The model showed overall significance, with both PLGA and sonication time influencing the response notably. Sonication time had a stronger impact compared to PLGA. Interaction and quadratic terms did not significantly affect the outcome, suggesting a mostly linear relationship (Table 10 and Figure 7).

Particle Size = 322.07 + 25.05*A – 49.53*B + 1.93A*B + $3.25*A^2 + 5.20*B^2$

Response 3: % CDR

This model was statistically significant, with PLGA and its quadratic effect playing a dominant role in the response.

Table 13: % CDR result of INM1-INM9

Time	INM1	INM2	INM3	INM4	INM5	INM6	INM7	INM8	INM9
0	0	0	0	0	0	0	0	0	0
1	4.7	5.7	6.7	5	5.8	6.5	2.8	4.1	7.1
2	10.7	15.1	15.1	12.3	15.1	15.2	7.5	10.5	16.6
3	12.7	18.2	18.2	16.1	21.1	19.8	11.8	15.5	23
4	14.4	19.1	20.9	19.5	26.3	24.6	16	21	29.4
5	16.8	21.6	23.1	23.2	31.5	29.8	20.2	27.4	36
6	18.9	24..97	27.3	27.8	39.3	36.2	25.2	34.4	43
7	21.1	31.2	33.5	32.8	48.8	44.4	29.6	41.9	48.6
8	25.3	39.9	38.9	36.7	56.7	55.4	32.8	49.1	55.5
12	49.5	62.5	66.5	61.7	73.3	71.5	52.2	69.3	69.7
24	80.7	83.7	93.3	87.7	89.3	85.5	79.8	89.8	86.4

Table 14: R^2 value of kinetics model of check-point batch

Model	R^2
Zero Order	0.9959
First Order	0.9853
Higuchi	0.8799
Hixon	0.9898
Korserneyer-Peppas	0.9463

The quadratic term of sonication time also contributed significantly, while the interaction between variables remained non-significant. This indicates that both linear and nonlinear effects of formulation factors influenced the response (Table 11 and Figure 8).

% CDR = 72.86 + 6.90*A + 2.63*B – 0.65*A*B – 6.03*A2 – 6.73*B2

Validation of Experimental Model

The predicted values and experimental values are given in Table 12 and Figure 9.

Evaluation of Ivacaftor Nanoparticles

Particle Size and PDI

The particle size and polydispersity index (PDI) values for various Ivacaftor nanoparticle batches demonstrated a range of particle sizes with relatively low PDI values, indicating uniformity and stability in most formulations. Among them, IN7 and IN8 showed the smallest particle sizes with narrow distribution, suggesting optimal formulation characteristics (Table 17 and Figure 10).

% Nanoparticle Yield, Drug Loading and Entrapment Efficiency

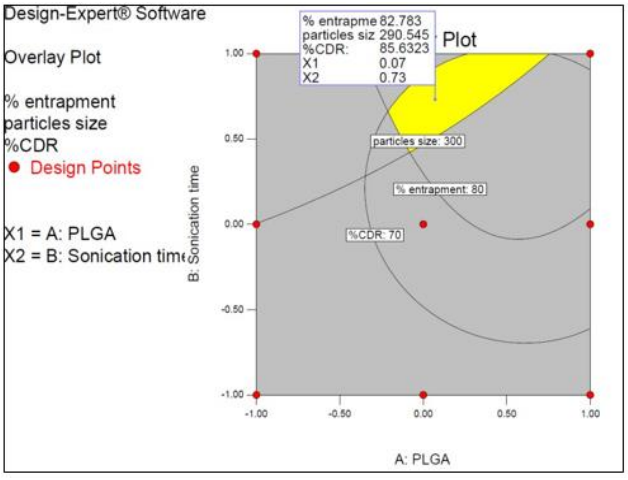

Figure 9: Overlay Plot

Table 15: Stability Study of optimized Ivacaftor-loaded nanoparticle

S. No	Parameters	Stability Conditions (25 ± 2 °C /65 % ± 5 %RH)	
		Initial	30 days
1	Particle Size	282.8	276.4
2	%EE	83.3	79.6
3	%CDR	89.8	86.9

Table 16: Particle Size and PDI of IN1 – IN9

Batch	Particle Size	PDI
IN1	356.5	0.327
IN2	362.9	0.613
IN3	417.5	0.211
IN4	310.6	0.258
IN5	330.9	0.668
IN6	331.2	0.107
IN7	244.1	0.301
IN8	282.8	0.112
IN9	312.8	0.303

The study results revealed notable differences in yield, drug loading, and entrapment efficiency among the formulations. While Batch F2 showed the highest yield, Batches F8 and F9 demonstrated superior drug loading and entrapment efficiency, identifying them as the most promising candidates for Ivacaftor delivery (Table 13).

SEM - Scanning Electron Microscopy

The grayscale image clearly illustrates the morphology of the synthesized nanoparticles, showing smooth, spherical particles with uniform size distribution. This consistency confirms the successful formulation process and structural integrity of the nanoparticles. Such uniform morphology is essential for reproducible drug delivery and supports the reliability of the preparation method used (Figure 11).

In-vitro Drug Release Study

The *in vitro* drug release study of Ivacaftor nanoparticles (INM1–INM9) revealed an initial burst followed by a sustained release phase, indicating effective controlled-release characteristics. Variations among batches highlighted the role of formulation factors, with INM5, INM6, and INM9 showing enhanced release profiles. INM3 exhibited the highest cumulative release, while INM7 showed the lowest, suggesting differences in matrix integrity and drug encapsulation efficiency (Figure 12 and Table 14).

Drug Release Kinetics

The drug release data best fit the Zero Order kinetic model, as indicated by the highest R^2 value, suggesting a constant drug release rate over time. Other models like First Order and Hixson-Crowell also showed good correlation, while the Higuchi and Korsmeyer-Peppas models demonstrated comparatively lower fit (Table 15).

Stability Study

The stability study of the Ivacaftor nanoparticle formulation under specified conditions showed minimal changes in particle size, entrapment efficiency, and cumulative drug release over 30 days. These slight reductions indicate good physical and chemical stability, with limited aggregation or drug loss. The formulation thus remains a viable candidate for sustained drug delivery (Table 16).

DISCUSSION

The study aimed to develop and optimize Ivacaftor-loaded PLGA nanoparticles to address the limitations of conventional oral delivery, primarily poor solubility and bioavailability. The preliminary screening of formulation

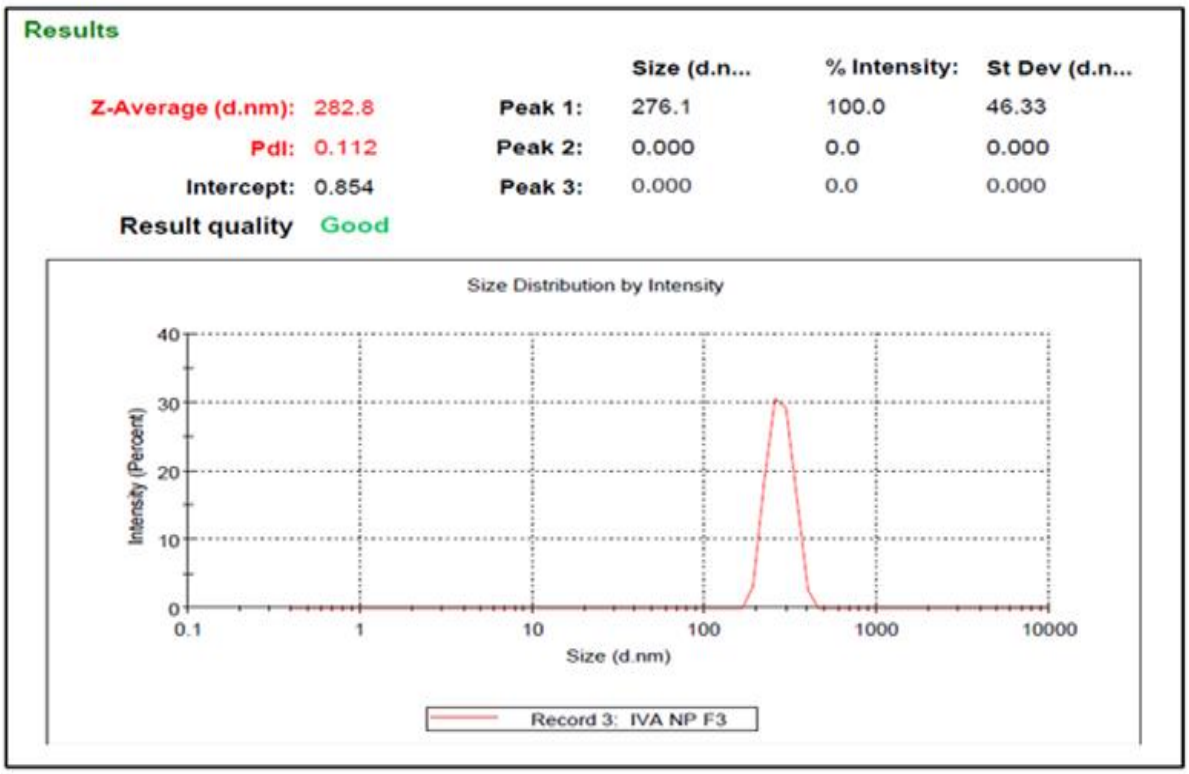

Figure 10: Particle Size of Check-Point Batch

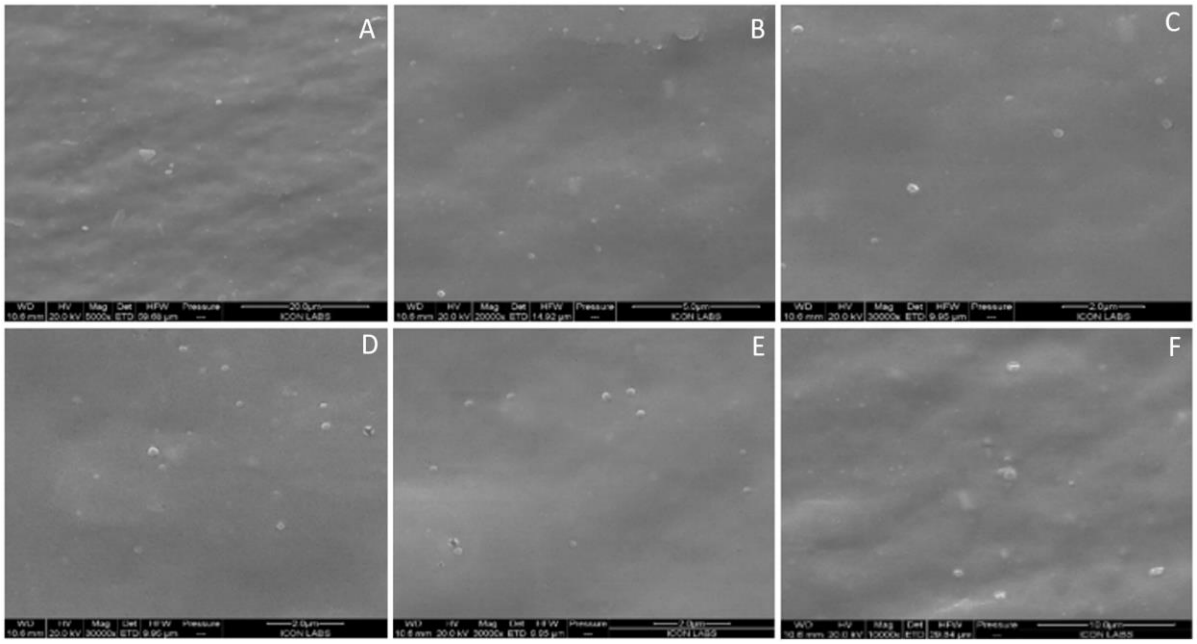

Figure 11: (A)-(F) Shows the size, shape, and morphology of nanoparticle

parameters, including the drug-to-polymer ratio, surfactant concentration, homogenization speed, and sonication amplitude, was critical in identifying the optimal conditions for nanoparticle synthesis. The 1:7 drug-to-polymer ratio provided the highest entrapment efficiency and favorable polydispersity index (PDI), indicating effective encapsulation and uniform particle distribution. Similarly, a surfactant concentration of 1% w/v resulted in nanoparticles with minimal particle size, enhancing their potential for pulmonary delivery.

The optimized formulation, labeled INM8, exhibited favorable characteristics including a particle size below 300 nm, high entrapment efficiency, and a controlled drug release profile. *In vitro* release studies showed an initial burst release followed by a sustained release phase, supporting the maintenance of therapeutic drug levels over an extended period. Notably, the release followed zero-order kinetics, indicating a steady release rate regardless of drug concentration—an ideal scenario for chronic conditions like cystic fibrosis, where consistent plasma levels are essential for therapeutic success.

FT-IR spectral analysis confirmed the chemical compatibility of Ivacaftor with PLGA and other formulation components, as no significant shifts or disappearance of major functional peaks were observed. This suggests the absence of chemical interactions and affirms the structural integrity of both the drug and polymer. Stability studies conducted under controlled conditions over 30 days showed negligible variation in particle size, drug entrapment, and cumulative release, indicating the formulation's robustness over time.

Morphological evaluation further revealed that the nanoparticles possessed a smooth, spherical surface with a uniform size distribution—attributes that are critical for predictable deposition and reproducible dosing, especially in pulmonary delivery. Overall, the results highlight the effectiveness of PLGA-based nanoparticles in improving the solubility and sustained delivery of Ivacaftor. Further *in vivo* evaluations are essential to confirm the pharmacokinetic profile and therapeutic potential of this delivery system in cystic fibrosis treatment.

CONCLUSION

Ivacaftor, a CFTR modulator, represents a significant advancement in the treatment of Cystic Fibrosis (CF), though its therapeutic potential is limited by poor oral solubility. To address this, Ivacaftor-loaded polymeric nanoparticles were developed using a single emulsion solvent evaporation technique, with PLGA as the biodegradable polymer, PVA as a stabilizer, and a solvent mix of ethanol and dichloromethane. The formulation process was refined through experimental design by adjusting polymer and surfactant concentrations, homogenization speed, and sonication conditions. The optimized formulation, INM8, exhibited desirable characteristics including nanoscale particle size, high drug entrapment, zero-order controlled release, and strong stability—making it well-suited for pulmonary delivery. Incorporation with mannitol enabled dry powder inhalation, offering good flowability and consistent dosing. Stability testing showed minimal variation, reinforcing its potential for sustained lung-targeted therapy. Further preclinical investigations are warranted to assess its pharmacokinetics, therapeutic efficacy, and safety profile. This strategy demonstrates the promise of polymeric nanoparticles in improving Ivacaftor delivery and presents a scalable approach for treating CF and similar chronic respiratory conditions.

Acknowledgements

Authors thank RDC cell of Parul university, Vadodara, Gujarat for providing Intermural research grant use of

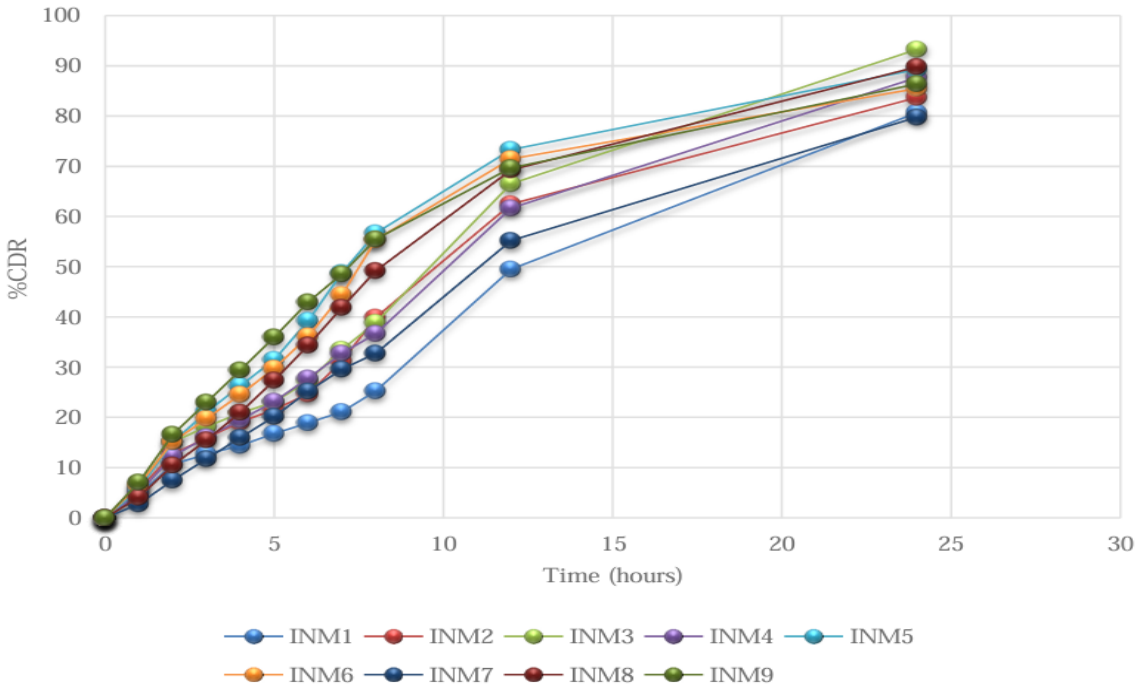

Figure 12: % CDR of INM1-INM9

instruments for this work. Authors also thank School of Pharmacy, Parul university, Vadodara, Gujarat for proving the chemicals, instrumentation, and necessary support for this work. Authors Dr.Lalit lata jha and Dr.Meenakshi Patel for their necessary follow-up.

AUTHORS CONTRIBUTIONS

Bhavesh Mali contributed to the conceptualization, design of experiments, visualization, investigation, data curation, interpretation of study outcomes. Dr.K.Sushma provided supervision, contributed to conceptualization, design of experiments, visualization, investigation, data curation, interpretation of study outcomes and participated in writing, reviewing, and editing. Himanshu Patel contributed to the interpretation of study outcomes, as well as writing, reviewing, and editing. Ms. Nidhi Raichura contributed for interpretation of analytical study outcomes and participated in review and editing of the final manuscript. All authors collaborated to ensure the integrity and quality of this research.

REFERENCES

1. Ivacaftor: Uses, interactions, mechanism of action | DrugBank Online [Internet].Drug Bank.Available from: https://go.drugbank.com/drugs/DB08820
2. Bylima TV, Bylim BV, Davydenkoa VE, Dmitrievna SS, Idzibagandova AS. Indazole-based privileged ligands in polypharmacology : Unlocking the ' undruggable ' membrane transporter landscape. J Med Pharm Chem Res. 2025;7(March):2596–629.
3. Castellani C, Cuppens H, Macek M Jr, Cassiman JJ, Kerem E, Durie P, et al. Consensus on the use and interpretation of cystic fibrosis mutation analysis in clinical practice. J Cyst Fibros [Internet]. 2008;7(3):179–96.
4. Rosenstein BJ, Cutting GR. The diagnosis of cystic fibrosis: A consensus statement. J Pediatr [Internet]. 1998;132(4):589–95.
5. Bhardwaj V, Hariharan S, Bala I, Lamprecht A, Kumar N, Panchagnula R. Pharmaceutical aspects of polymeric nanoparticles for oral delivery. Journal of Biomedical And Nanotechnology. 2005; 1: 1-23.
6. Rajput N. Methods of preparation of nanoparticles-a review. International Journal of Advances in Engineering & Technology. 2015;7(6):1806.
7. Ball RL, Bajaj P, Whitehead KA. Achieving long-term stability of lipid nanoparticles: examining the effect of pH, temperature, and lyophilization. International journal of nanomedicine. 2017 Dec 30:305-15.
8. Umerska A, Gaucher C, Oyarzun-Ampuero F, Fries-Raeth I, Colin F, Villamizar-Sarmiento M, et al. Polymeric Nanoparticles for Increasing Oral Bioavailability of Curcumin. Antioxidants. 2018 Mar 24;7(4):46.
9. Sadik AF, Mostafa EM, El-sherif RM. Advanced Functionalization of Polysulfone Membranes with Green-Synthesized Silica (Si) and Silica-Silver (Si-Ag) Nanocomposites for Water Desalination and Environmental Applications. Asian J Green Chem. 2025;9:716–37.
10. Varuna U, Venkata N, Vidiyala N, Sunkishala P. Bio-Inspired Green Synthesis of Nanoparticles for Psoriasis Treatment : A Review of Current Status and Future Directions. Asian J Green Chem. 2025;9:373–403.
11. Bhattacharya S, Anjum MM, Patel KK. Gemcitabine cationic polymeric nanoparticles against ovarian cancer: formulation, characterization, and targeted drug delivery. Drug Delivery. 2022 Apr 1;29(1):1060–74.
12. Modena MM, Rühle B, Burg TP, Wuttke S. Nanoparticle characterization: what to measure?. Advanced Materials. 2019 Aug;31(32):1901556.
13. Mourdikoudis S, Pallares RM, Thanh NT. Characterization techniques for nanoparticles: comparison and complementarity upon studying nanoparticle properties. Nanoscale. 2018;10(27):12871-934.
14. Prashant T, Ashish S, Prabhakar P, Dipak G. Quercetin-Loaded Graphene Oxide Nanoparticles: Synthesis, Optimization, And Evaluation for Breast Cancer Treatment. International Journal of Applied Pharmaceutics. 2025 May 7;243–51.
15. Sakhi M, Khan A, Iqbal Z, Khan I, Raza A, Ullah A, et al. Design and Characterization of Paclitaxel-Loaded Polymeric Nanoparticles Decorated With Trastuzumab for the Effective Treatment of Breast Cancer. Frontiers in Pharmacology. 2022 Mar 14;13.
16. Rapolu K, Muvvala S. Optimization and Characterization of Brinzolamide Loaded Biodegradable, Amphiphilic Poly-caprolactone-Polyethylene Glycol-Poly-Caprolactone (5000-1000-5000) Tri-block Co-polymeric Carriers as Long-Acting Intravitreal Drug Delivery Vehicle for Glaucoma Therapy. Adv J Chem Sect A. 2025;8(3):639–66.
17. Alhussein ABA, Gaaz TS, Jaaz AH, Alsultany FH, Kadhum AAH, Al-Amiery AA, et al. Preparation of Nanoparticles Loaded by Dimethyl Fumarate and Their Physical and Chemical Properties Study. Adv J Chem Sect A. 2025;8(1):194–208.
18. Salman SS. Green Synthesis , Analysis , and Characterization of Nano-silver- Based Conyza Canadensis (SYN : Erigeron Canadensis) Extract. Chem Methodol. 2024;8:856–73.
19. Nair RS, Morris A, Billa N, Leong CO. An Evaluation of Curcumin- Encapsulated Chitosan Nanoparticles for Transdermal Delivery. AAPS PharmSciTech. 2019 Jan 10;20(2).
20. Awwad AM, Salem NM, Marwa Aqarbeh, Abdulaziz FM. Green synthesis, characterization of silver sulfide nanoparticles and antibacterial activity evaluation. Zenodo (CERN European Organization for Nuclear Research). 2020 Jan 1;
21. Prohit PV, Pakhare PS, Pawar VB, Dandade SS, Waghmare MS, Shaikh FA, et al. Formulation and Comparative Evaluation of Naproxen-Based Transdermal Gels. J Pharm Sci Comput Chem. 2025;1(2):83–105.
22. Yothi D, Priya S, James Jp. Development and Optimization Of Polymeric Nanoparticles Of Glycyrrhizin: Physicochemical Characterization And

Antioxidant Activity. International Journal of Applied Pharmaceutics. 2024 Jan 7;166–71.
23. Yadav Nk, Mazumder R, Rani A, Kumar A. Current Perspectives On Using Nanoparticles for Diabetes Management. International Journal of Applied Pharmaceutics. 2024 Sep 7;38–45